Evaluation of RTK-GPS Performance with Low-cost Single-frequency GPS Receivers

Tomoji Takasu, Akio Yasuda
Tokyo University of Marine Science and Technology, Japan
ttaka@gpspp.sakura.ne.jp

BIOGRAPHY

Tomoji Takasu is a researcher in Funai Laboratory of Satellite Navigation at Tokyo University of Marine Science and Technology. He was working for developments of satellite systems at NEC Aerospace systems Ltd. from 1984 to 1997. He is currently involved in the research and development of precise positioning algorithms with GPS/GNSS, including PPP, RTK-GPS and INS/GPS integration.

Akio Yasuda graduated in 1966 from Dept. of Electrical Eng., Nagoya Institute of Technology, and obtained Dr. of Eng. degree from Nagoya University, and worked at Nagoya University and at Tokyo University of Mercantile Marine. Since 2004, he was Prof. at Tokyo University of Marine Science and Technology. He is currently conductor of Funai laboratory of Satellite Navigation. He was engaged in research on development of marine wave meter, BS and GMS reception onboard, regional positioning system with geostationary satellites. His concerning of GPS started in 1987. He is presently conducting the researches on multipath mitigation, analysis of ionospherical delay, improvement of RTK-GPS algorism, and the other GPS related subjects. He is a member of IEICE (fellow), Japan Inst. Navigation, ION and IEEE.

ABSTRACT

It has been considered that low-cost single-frequency GPS antenna and receiver are not applicable to precise positioning by RTK-GPS. In this study, to confirm the RTK-GPS performance with such low-cost antenna and receiver, some field tests were conducted. At first, by using the field calibration method, the antenna PCV (phase center variation), carrier-phase multipath and code multipath were measured with various combination of antennas and receivers. Next, the RTK-GPS performance, including the positioning accuracy, fix-rate and TTFF for ambiguity resolution, was evaluated. According to the results of the experiments, these antenna and receiver are feasible for RTK-GPS but some attention should be paid for practical performance.

INTRODUCTION

RTK-GPS (realtime kinematic GPS) is one of the most precise positioning technologies, with which users can obtain cm-level accuracy of the position in real-time by processing carrier-phase measurements of GPS signals. It is generally considered that geodetic-grade dual-frequency GPS antenna and receiver are necessary to achieve practical performance of RTK-GPS. Low-cost single-frequency GPS antenna and receiver are not applicable to RTK-GPS because of their poor performance. However, geodetic-grade antenna and receiver have been still expensive compared to consumer-grade ones. This is one of the reasons why RTK-GPS is still not popular and is utilized only for limited applications like land survey. If the low-cost antenna and receiver were available for RTK-GPS, larger number of users, who need more precise positions, would intend to use the technique. More applications of RTK-GPS, currently not applicable due to cost issues, would become practical. The objective of this study is to evaluate the performance of RTK-GPS with low-cost single-frequency antenna and receiver and to clarify issues to apply them to RTK-GPS.

EVALUATION OF ANTENNAS AND RECEIVERS BY FIELD CALIBRATION

The field calibration is often used for evaluation of GPS antennas. According to the technique, a target antenna is mounted on a field with good sky view. A reference antenna is placed in the vicinity of the target as well. Both of the antennas are connected to receivers to record raw measurement data of GPS signals in a certain period typically 24 hours. Recorded data are processed together by a post-mission analysis to obtain the antenna phase center position and PCV. In this study, some field tests were conducted to evaluate the performances of low-cost antenna and receiver with the method. In addition to the antenna phase center position and PCV, carrier-phase multipaths and code multipaths were also extracted in the same time. By using dual-frequency antenna and receiver as reference, the characteristics of single-frequency antenna and receiver were obtained. Figure 1 shows the

configuration of the field test. The target antenna was mounted on a ground-plane of 21 cm diameter to suppress multipaths. The baseline length between the target and the reference antennas was approximately 1 m. For each combination of antenna and receiver, raw GPS measurement data are sampled at the rate of 1 Hz for 24 hours. The recorded raw measurement data were analyzed to evaluate the performance of antenna and receiver by the following way.

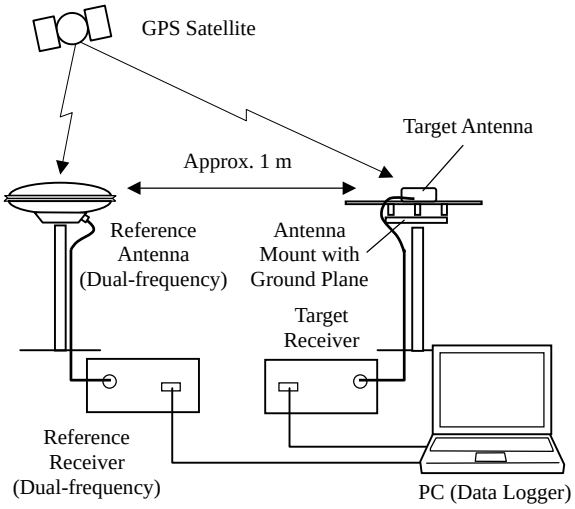

Figure 1. Configuration for evaluation of the antenna and receiver performance by field test

ESTIMATION OF ANTENNA PHASE CENTER/ VARIATION AND CARRIER-PHASE MULTIPATH

By using EKF (extended Kalman filter) [1], a state vector $\boldsymbol{x}$ and its covariance matrix $\boldsymbol{P}$ can be estimated by:

$$\begin{aligned}
&\hat{\boldsymbol{x}}_k(+) = \hat{\boldsymbol{x}}_k(-) + \boldsymbol{K}_k \boldsymbol{v}(\hat{\boldsymbol{x}}_k(-)) \\
&\boldsymbol{P}_k(+) = (\boldsymbol{I} - \boldsymbol{K}_k \boldsymbol{H}(\hat{\boldsymbol{x}}_k(-)))\boldsymbol{P}_k(-) \\
&\boldsymbol{K}_k = \boldsymbol{P}_k(-)\boldsymbol{H}(\hat{\boldsymbol{x}}_k(-))(\boldsymbol{H}(\hat{\boldsymbol{x}}_k(-))\boldsymbol{P}_k(-)\boldsymbol{H}(\hat{\boldsymbol{x}}_k(-))^T) + \boldsymbol{R})^{-1}
\end{aligned} \tag{1}$$

where $\boldsymbol{v}(\boldsymbol{x})$, $\boldsymbol{H}(\boldsymbol{x})$ and $\boldsymbol{R}$ are the residual vector, the matrix of partial derivatives and the covariance matrix of measurement errors, respectively. Assuming the system model stationary and no system noise, the time update from t_k to t_{k+1} of EKF is just expressed as:

$$\hat{\boldsymbol{x}}_{k+1}(-) = \hat{\boldsymbol{x}}_k(+), \quad \boldsymbol{P}_{k+1}(-) = \boldsymbol{P}_k(+) \tag{2}$$

At first, the antenna phase center position is determined by the following way. The state vector is defined as:

$$\boldsymbol{x} = (\boldsymbol{r}_u^{\,t}, N_{ur}^1, N_{ur}^2, ..., N_{ur}^m)^T \tag{3}$$

With single-differenced residuals of carrier-phase measurements, the double-differenced residuals, the partial derivatives and the covariance of measurement errors are expressed as:

$$\boldsymbol{v}_k(\boldsymbol{x}) = \boldsymbol{D}\boldsymbol{v}_{ur,k}(\boldsymbol{x}) \;\; \boldsymbol{H}(\boldsymbol{x}) = \boldsymbol{D}\boldsymbol{H}_{ur}(\boldsymbol{x}), \; \boldsymbol{R} = \boldsymbol{D}\boldsymbol{R}_{ur}\boldsymbol{D}^T \tag{4}$$

$$\boldsymbol{v}_{ur}(\boldsymbol{x}) = \begin{pmatrix} \lambda\phi_{ur}^1 - (\rho_{ur,k}^1 + N_{ur}^1) \\ \lambda\phi_{ur}^2 - (\rho_{ur}^2 + N_{ur}^2) \\ \vdots \\ \lambda\phi_{ur}^m - (\rho_{ur}^m + N_{ur}^m) \end{pmatrix}$$

$$\boldsymbol{H}_{ur}(\boldsymbol{x}) = \begin{pmatrix} -\boldsymbol{e}_u^1 & 1 & 0 & \cdots & 0 \\ -\boldsymbol{e}_u^2 & 0 & 1 & \cdots & 0 \\ \vdots & \vdots & \vdots & \ddots & \vdots \\ -\boldsymbol{e}_u^m & 0 & 0 & \cdots & 1 \end{pmatrix}$$

$$\boldsymbol{R}_{ur} = \mathrm{diag}(2\sigma_\phi{}^2, 2\sigma_\phi{}^2, ..., 2\sigma_\phi{}^2)$$

$$\rho_{ur}^i = \left\| \boldsymbol{r}^i - \boldsymbol{r}_u \right\| - \left\| \boldsymbol{r}^i - \boldsymbol{r}_r \right\|, \quad \boldsymbol{e}_u^i = (\boldsymbol{r}^i - \boldsymbol{r}_u) / \left\| \boldsymbol{r}^i - \boldsymbol{r}_u \right\|$$

where:

- $()_{ur}$: single-difference between target and reference antennas
- $\boldsymbol{r}_u$: target antenna phase center position (m)
- $\boldsymbol{r}_r$: reference antenna phase center position (m)
- $\boldsymbol{r}^i$: satellite i position (m)
- λ : carrier wave length (m)
- ϕ_u^i : carrier-phase measurement (cycle)
- ρ_u^i : geometric range (m)
- N_u^i : carrier-phase ambiguity (m)
- $\boldsymbol{e}_u^i$: LOS (line of sight) vector
- σ_ϕ : standard deviation of carrier-phase measurement error (m)

$$\boldsymbol{D} = \begin{pmatrix} 1 & -1 & 0 & \cdots & 0 \\ 1 & 0 & -1 & \cdots & 0 \\ \vdots & \vdots & \vdots & \ddots & \vdots \\ 1 & 0 & 0 & \cdots & -1 \end{pmatrix} : \text{single-differencing matrix}$$

By solving the EKF formula (1), (2) with equation (4), the phase center position of the target antenna is obtained as the final solution of $\hat{\boldsymbol{r}}_u$. In this case, the carrier-phase ambiguities are not fixed to integers.

In the next step, the target antenna PCV is estimated. The state vector is defined as:

$$\boldsymbol{x} = (N_{ur}^1, N_{ur}^2, ..., N_{ur}^m, \boldsymbol{c}^T)^T \tag{5}$$

where $\boldsymbol{c}$ is a coefficient vector defined as:

$$\boldsymbol{c} = (c_{10}, c_{11c}, c_{11s}, c_{20}, c_{21c}, c_{21s}, c_{22c}, c_{22s}, c_{30}, ...)^T \tag{6}$$

With the coefficients and spherical harmonic functions, the target antenna PCV $\Delta\phi$ is written as:

$$\begin{aligned}
&\Delta\phi(a,e) = \boldsymbol{c}^T \boldsymbol{Y}(a,e) \qquad (7)\\
&\boldsymbol{Y}(a,e) = (Y_{10}(a,e), Y_{11c}(a,e), Y_{11s}(a,e), Y_{20}(a,e), Y_{21c}(a,e),\\
&\qquad Y_{21s}(a,e), Y_{22c}(a,e), Y_{22s}(a,e), Y_{30}(a,e), \ldots)^T\\
&Y_{n0}(a,e) = \overline{P}_{n0}(-\cos(2e))\\
&Y_{nm\{c|s\}}(a,e) = \overline{P}_{nm}(-\cos(2e))\{\cos(ma) \mid \sin(ma)\})
\end{aligned}$$

where:

a, e : azimuth and elevation angle (rad)

$Y_{nm\{s|c\}}$: (n,m) spherical harmonic function

$\overline{P}_{nm}$: (n,m) normalized Legendre function

To estimate the antenna PCV, the same formula is used as equation (4) but $\boldsymbol{v}_{ur}(\boldsymbol{x})$ and $\boldsymbol{H}_{ur}(\boldsymbol{x})$ are replaced by:

$$\boldsymbol{v}_{ur}(\boldsymbol{x}) = \begin{pmatrix} \lambda\phi_{ur}^1 - (\rho_{ur}^1 + N_{ur}^1 + \Delta\phi(a_u^1, e_u^1)) \\ \lambda\phi_{ur}^2 - (\rho_{ur}^2 + N_{ur}^2 + \Delta\phi(a_u^2, e_u^2)) \\ \vdots \\ \lambda\phi_{ur}^m - (\rho_{ur}^m + N_{ur}^m + \Delta\phi(a_u^m, e_u^m)) \end{pmatrix}$$

$$\boldsymbol{H}_{ur}(\boldsymbol{x}) = \begin{pmatrix} 1 & 0 & \cdots & 0 & \boldsymbol{Y}(a_u^1, e_u^1)^T \\ 0 & 1 & \cdots & 0 & \boldsymbol{Y}(a_u^2, e_u^2)^T \\ \vdots & \vdots & \ddots & \vdots & \vdots \\ 0 & 0 & \cdots & 1 & \boldsymbol{Y}(a_u^m, e_u^m)^T \end{pmatrix}$$

where the phase center position $\boldsymbol{r}_u$ of the target antenna is fixed to the value determined in the first step. By solving the EKF formulas with these equations, the target antenna PCV is obtained as the final solution of $\boldsymbol{c}$. Note that the estimated antenna PCV is relative value to the reference antenna. To obtain the absolute antenna PCV, a "zero-offset" type antenna is used for the reference or corrections are made with the reference antenna PCV determined by the other way.

In company with the PCV determined, the carrier-phase multipaths can be extracted. Assuming the sum of the residuals equals to zero, the single-differenced post-fit residuals of the measurement update step of EKF at t_k is written as:

$$\boldsymbol{m}_{ur,k} = (m_{ur,k}^1, m_{ur,k}^2, \ldots, m_{ur,k}^m)^T = \boldsymbol{v}_k(\hat{\boldsymbol{x}}_k(+)) - \overline{v}_k \qquad (8)$$

where $\overline{v}_k$ is the average of the post-fit residuals of the double-differenced carrier-phase measurements. The residuals consist of the carrier-phase multipaths and carrier tracking noises in the receiver. Assuming that the carrier tracking noises are white, a filter reduces the noises. Finally, by applying a simple moving-average filter, the carrier-phase multipath for satellite i at t_k can be approximated by:

$$\begin{aligned}
\tilde{m}_{ur,k}^i \approx (&m_{ur,k-n}^i + m_{ur,k-n+1}^i + \ldots +\\
&m_{ur,k+n-1}^i + m_{ur,k+n}^i)/(2n+1)
\end{aligned} \qquad (9)$$

where $(2n+1)$ is the window size of the moving-average filter. The estimated multipaths represent the single-difference between the target and reference antenna.

ESTIMATION OF CODE MULTIPATH

By eliminating the ionospheric delay term with dual-frequency carrier-phase measurements of the reference antenna in the vicinity of the target antenna, the code multipaths can be extracted as well as the carrier-phase multipaths. The L_1 ionospheric delay plus bias is estimated with the geometry-free LC (linear-combination) of the dual-frequency carrier-phase measurements of the reference antenna at t_k by:

$$L_{r,k}^i = -(\lambda_{L1}\phi_{r,k,L1}^i - \lambda_{L2}\phi_{r,k,L2}^i)/(1 - {f_{L1}}^2 / {f_{L2}}^2) \qquad (10)$$

where:

L_r^i : L_1 ionospheric delay plus bias (m)

f_{Lj} : L_j carrier frequency (Hz)

By subtracting the averaged ionospheric delay plus bias in an arc, the L_1 ionospheric delay variation is obtained by:

$$\boldsymbol{I}_r^i = (I_{r,1}^i, I_{r,2}^i, \ldots, I_{r,n}^i)^T = (L_{r,1}^i, L_{r,2}^i, \ldots, L_{r,n}^i)^T - \overline{L_r^i} \qquad (11)$$

By neglecting the errors of carrier-phase measurements, the variation of code multipath plus code tracking noise of the target antenna is estimated as the code minus carrier-phase LC corrected with the estimated ionospheric delay variation by:

$$\delta_{r,Lj,k}^i = P_{r,Lj,k}^i - \lambda_{Lj}\phi_{r,Lj,k}^i - 2{f_{Lj}}^2 / {f_{L1}}^2 I_{r,k}^i \qquad (12)$$

Assuming the sum of the code multipath plus the receiver noises in the arc equal to zero, the bias is eliminated by subtracting the average in the arc as:

$$M_{r,Lj,k}^i = \delta_{r,Lj,k}^i - \overline{\delta}_{r,Lj}^i \qquad (13)$$

As well as the carrier-phase multipath, by reducing the code noises with the moving-average filter, the final code multipath for satellite i at t_k is obtained by:

$$\begin{aligned}
\tilde{M}_{ur,Lj,k}^i \approx (&M_{r,Lj,k-n}^i + M_{r,Lj,k-n+1}^i + \ldots\\
&+ M_{r,Lj,k+n-1}^i + M_{r,Lj,k+n}^i)/(2n+1)
\end{aligned} \qquad (14)$$

ANALYSIS TOOL: ANTTOOL

To analyze recorded raw GPS measurement data for evaluation of antenna and receiver performance, we developed an analysis tool called ANTTOOL, which implements the estimation of the antenna phase center position and PCV and the extraction of carrier-phase and code multipaths described above. ANTTOOL is written as Matlab m-files and inputs standard RINEX observation data and navigation messages for both of target and reference receivers. It can also generate some plots representing analysis results. ANTTOOL is freely available and is able to be used according to GPLv3 license. For details, refer [2].

EVALUATION OF RTK-GPS PERFORMANCE

In addition to the antenna and receiver performance, the RTK-GPS performance was evaluated with low-cost antenna and receiver. The performance includes the rate of resolved and validated integer ambiguities and the ratio of proper solutions, accuracy of fixed solutions and TTFF (time-to-first-fix) with ambiguity resolution. To evaluate them, we employed a precise positioning application and library package RTKLIB ver. 2.1.0 developed by the authors [3]. By using the post-mission baseline analysis of RTKLIB, the raw GPS measurement data of the target and reference receiver were processed by the single-frequency kinematic mode, that was the same condition as RTK-GPS. The carrier-phase ambiguities were resolved as an ILS (integer least square) problem by a well-known efficient search strategy LAMBDA and its extension MLAMBDA. The resolved integer ambiguity was validated by a simple ratio-test with the threshold value of 3. The solutions were compared to the reference position, which was obtained by 24 hours static baseline-analysis with a nearest reference station. The station coordinate was already determined within the cm-level accuracy in the ITRF frame. The ratio of properly resolved ambiguity was obtained by counting the solutions with the errors under 10 cm. To get the time to first fix, by sliding the starting time every 10 s in 24 hours, the first fix time after starting time was measured.

RESULTS AND CONSIDERATIONS

Table 1 lists the evaluated consumer-grade single-frequency antennas and receivers in this study. This table includes dual-frequency geodetic-grade antenna and receiver for the references as well. Figure 4, 5 and 6 show the detailed results of the performance evaluation with major combinations of antennas and receivers in Table 1, as antenna PCV, carrier-phase multipaths and code multipaths, respectively. Figure 2 summarizes the comparison of various antennas with the same receiver as RMS of carrier-phase and code multipaths. Figure 3 shows the comparison of receivers as well. Figure 5 and 6 show the evaluation results of RTK-GPS performance

Table 1. Evaluated antennas (upper) and receivers (lower) (*italic*: geodetic-grade)

Vendor	Antenna	Objective	Freq.	Type	Active/ Passive	LNA Gain	LNA NF	Size (mm)	weight (g)	Price	Note
u-blox	ANN-MS	General	L1	Patch	Active	27dB	1.5dB	40ϕ×48×13	105	$31	
Aero Antenna	AT575	General	L1	Patch	Active	12dB	?	53ϕ×13	113	$200	
AntCom	4G15A2-XS-3	Mini-Arinc Airborne	L1	Patch?	Active	?	?	55×86×17	?	$194	
Micro Pulse	2335TB	Vehicle Tracking	L1	Patch	Active	26dB	<2.5dB	65ϕ×12	28	$47	
Pioneer	GPS-M1ZZ Ant	General	L1	Patch	Active	?	?	31×35×12	?	?	
Trimble	Bullet III	General	L1	?	Active	35dB	<3.3dB	78ϕ×66	170	$125	
NovAtel	*GPS-702-GG*	*Geodetic/ Reference*	*L1/L2*	*Pinwheel*	*Active*	*29dB*	*2.0dB*	*185ϕ×69*	*500*	*$995*	Reference

Vendor	Receiver	Objective	Freq.	# of Channel	Max Rate	DGPS	Output	Size (mm)	Price	Note
u-blox	AEK-4T	General/ Timing	L1	16ch	4Hz/ 10Hz *1	SBAS/ RTCM	NMEA/ Binary	17×22×3 (Module)	$179 (Module)	
u-blox	EVK-5H	General	L1	50ch	4Hz/ 10Hz *1	SBAS/ RTCM	NMEA/ Binary *3	17×22×3 (Module)	$99 (Module)	
NovAtel	Superstart II (OEM Board)	Genaral	L1	12ch	1Hz/ 5Hz *2	SBAS/ RTCM	NMEA/ Binary	71×46×13	$165	
Hemisphere	Crescent (OEM Board)	General/ RTK-GPS	L1	12ch	1Hz/ 20Hz *2	SBAS/ RTCM	NMEA/ Binary	71×40×12	$285	
NovAtel	*OEMV-3*	*Geodetic/ Reference*	*L1/L2*	*24ch*	*20Hz*	*SBAS/ RTCM*	*NMEA/ Binary*	*185×160×71*	*$7,995 *4*	Reference

*, *1 Raw Measurement, *2 Optional, *3 F/W ver. 3.00, *4 No RTK Option*

with the same combinations, as the time series of east/north/up position errors and TTFF with ambiguity resolution. Table 2 summarizes the RTK-GPS performance. According to these results, the difference of the antenna performances is large between geodetic-grade and consumer-grade, especially for the phase center stability and code multipath. Generally, code multipath much affects to the performance of the RTK-GPS initialization. To improve TTFF, it might be effective to replace a low-cost antenna with geodetic-grade one. By contrast, the difference of receivers is not so large. The

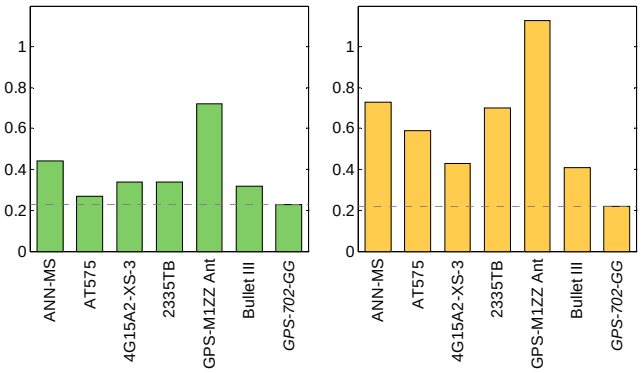

Figure 2. Comparison of antennas with the same receiver, phase multipath (cm) (left) and code multipath (m) (right)

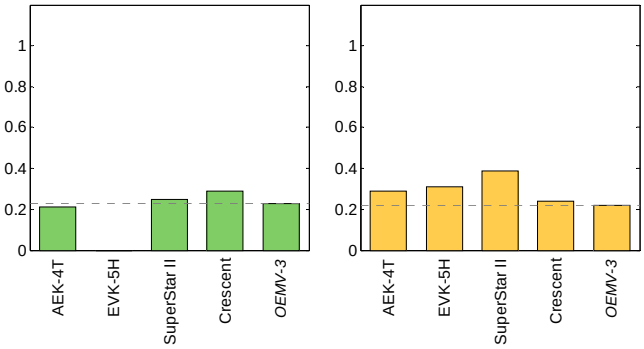

Figure 3. Comparison of receivers with the same antenna, phase multipath (cm) (left) and code multipath (m) (right)

carrier-phase multipath level of consumer-grade receivers is almost same as geodetic-grade. Therefore, the positioning accuracy of RTK-GPS would be sufficient even with consumer-grade receiver. Dual-frequency receivers, however, have an advantage of much shorter time of ambiguity resolution, ideally instantaneous. The results of TTFF test indicate that at least a few minutes are necessary for the first fix with a single-frequency receiver. So, in the environment with many cycle slips like for mobile vehicle navigation, a dual-frequency receiver is still necessary. Though, for the application with continuous observation like crustal deformation monitoring, low-cost single-frequency receiver could be applicable for short baseline RTK-GPS.

CONCLUSIONS

In this study, The RTK-GPS performance with low-cost single-frequency antenna and receiver were evaluated by some field tests. According to the results of the experiments, it is feasible to apply consumer-grade antenna and receiver to RTK-GPS. With a low-cost antenna, however, performance degradation is large, so replacing it with a geodetic-grade antenna is much effective to improve the performance. By contrast, as to receivers, the performance difference is smaller between the consumer-grade and the geodetic-grade.

REFERENCES

[1] A.Gelb ed., Applied Optimal Estimation, The M.I.T. Press, London, 1974

[2] GPS L1 Antenna/Receiver Evaluation - Analysis Tool. URL: *http://gpspp.sakura.ne.jp/anteva/anttool.htm*

[3] T.Takasu et al., N.Kubo and A.Yasuda, Development, evaluation and application of RTKLIB: A program library for RTK-GPS, GPS/GNSS symposium 2007, Tokyo, Japan, 20-22 November, 2007 (in Japanese)

Table 2. Summary of RTK-GPS performances (*italic*: geodetic-grade)

Rover		Ambiguity Resolution		RMS Error of Fixed Solution			TTFF with AR		
Antenna	Receiver	Fix-Rate	Success- Rate	E-W	N-S	U-D	Mean	95%	Max
ANN-MS	*OEMV-3*	94.8 %	99.8 %	0.47 cm	0.53 cm	1.09 cm	968.5 s	3010.0 s	6310.0 s
AT575	*OEMV-3*	98.3 %	99.7 %	0.34 cm	0.42 cm	0.90 cm	436.7 s	1370.0 s	3500.0 s
4G15A2-XS-3	*OEMV-3*	96.8 %	99.8 %	0.41 cm	0.49 cm	1.12 cm	514.4 s	1650.0 s	3260.0 s
2335TB	*OEMV-3*	98.4 %	99.6 %	0.38 cm	0.47 cm	1.10 cm	535.8 s	1550.0 s	2940.0 s
GPS-M1ZZ Ant	*OEMV-3*	97.1 %	99.5 %	0.45 cm	0.56 cm	1.15 cm	983.2 s	3910.0 s	6600.0 s
Bullet III	*OEMV-3*	99.4 %	99.8 %	0.30 cm	0.47 cm	1.04 cm	256.8 s	816.0 s	2200.0 s
GPS-702-GG	AEK-4T	99.9 %	100.0 %	0.26 cm	0.34 cm	0.81 cm	131.2 s	490.0 s	1200.0 s
GPS-702-GG	EVK-5H	0.0 %	0.0 %	-	-	-	-	-	-
GPS-702-GG	Superstar II	99.6 %	100.0 %	0.28 cm	0.39 cm	0.85 cm	490.1 s	2000.0 s	4280.0 s
GPS-702-GG	Crescent	99.5 %	100.0 %	0.33 cm	0.46 cm	0.99 cm	183.1 s	730.0 s	1750.0 s
ANN-MS	AEK-4T	98.7 %	100.0 %	0.39 cm	0.59 cm	1.08 cm	652.8 s	1840.0 s	3490.0 s
ANN-MS	EVK-5H	0.0 %	0.0 %	-	-	-	-	-	-
ANN-MS	Superstar II	98.4 %	100.0 %	0.44 cm	0.65 cm	1.23 cm	1033.3 s	2890.0 s	4570.0 s
ANN-MS	Crescent	96.5 %	100.0 %	0.44 cm	0.60 cm	1.37 cm	758.0 s	2270.0 s	5020.0 s
GPS-702-GG	*OEMV-3*	99.8 %	100.0%	0.26 cm	0.36 cm	0.77 cm	132.7 s	630.0 s	1240.0 s

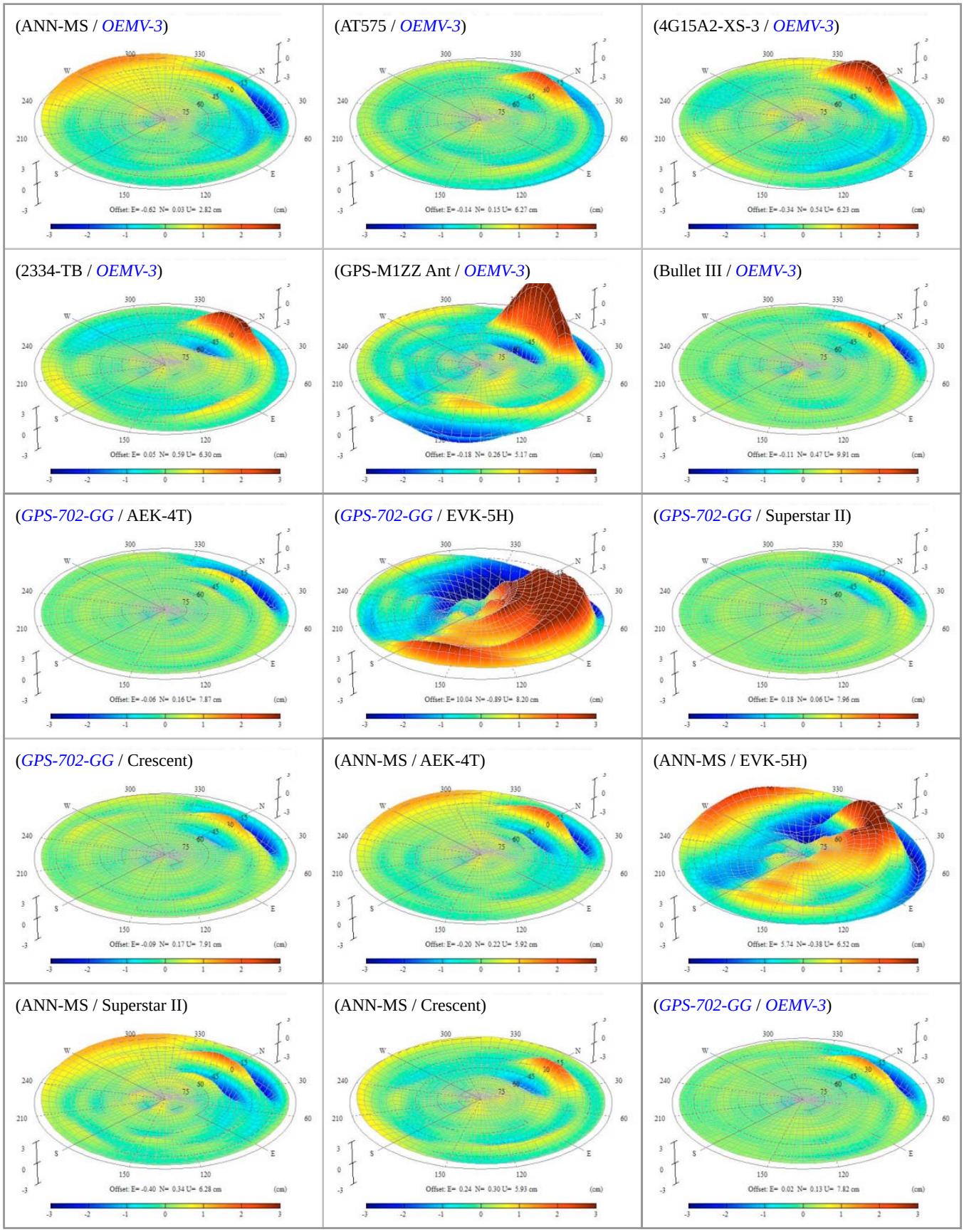

Figure 4. 3D-skyplot of antenna PCV (antenna / receiver, *italic*: geodetic-grade)
(upper right - lower left: north - south directions. note that anomalies in north areas are cased by outage of satellite path)

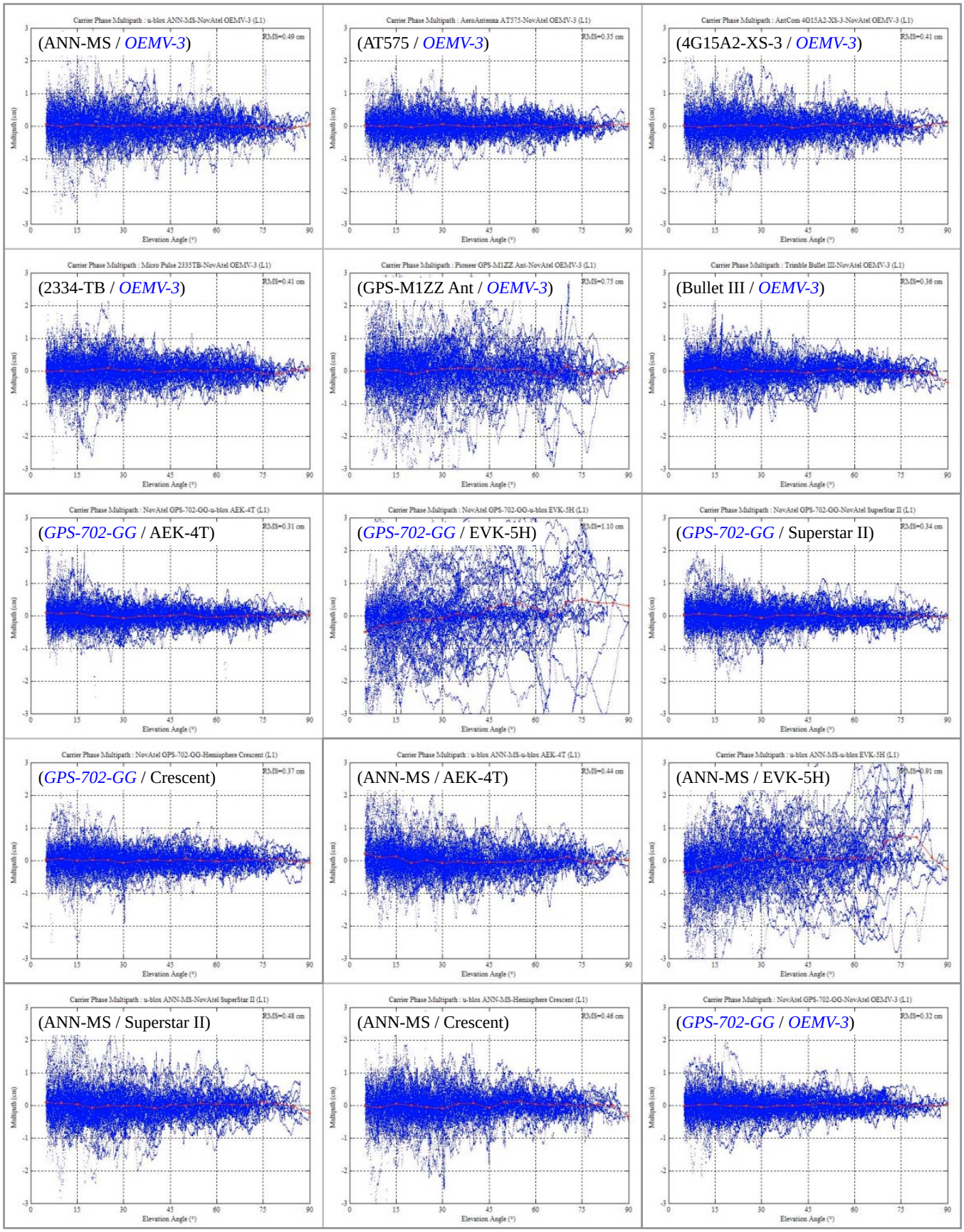

Figure 5. Carrier-phase multipaths (antenna / receiver, *italic*: geodetic-grade)
(x-axis: elevation angle in the range of 0 - 90°, y-axis: carrier-phase multipath in the range of -3 to 3 cm)

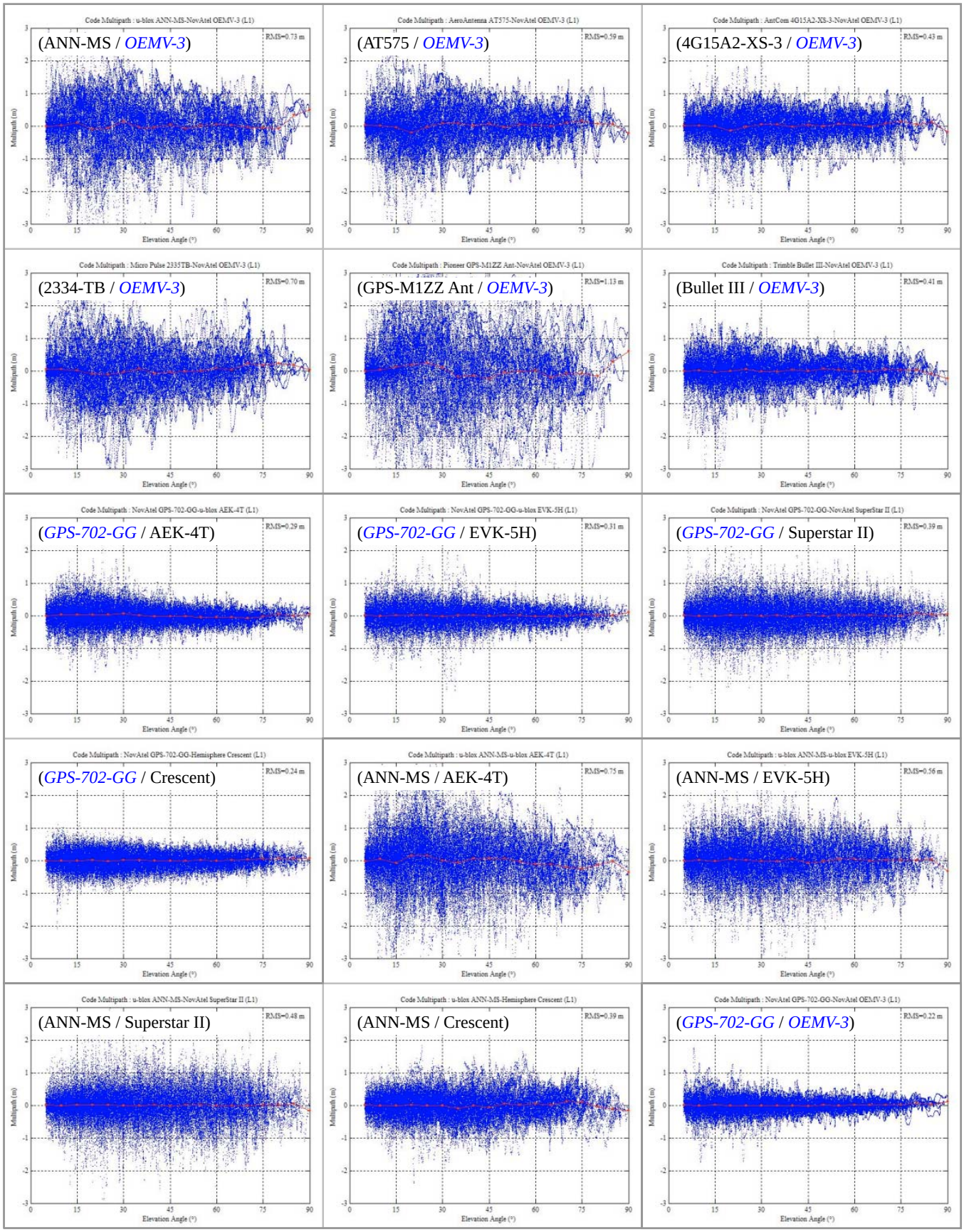

Figure 6. Code multipaths (antenna / receiver, *italic*: geodetic-grade)
(x-axis: elevation angle in the range of 0 - 90°, y-axis: code multipath in the range of -3 to 3 m)

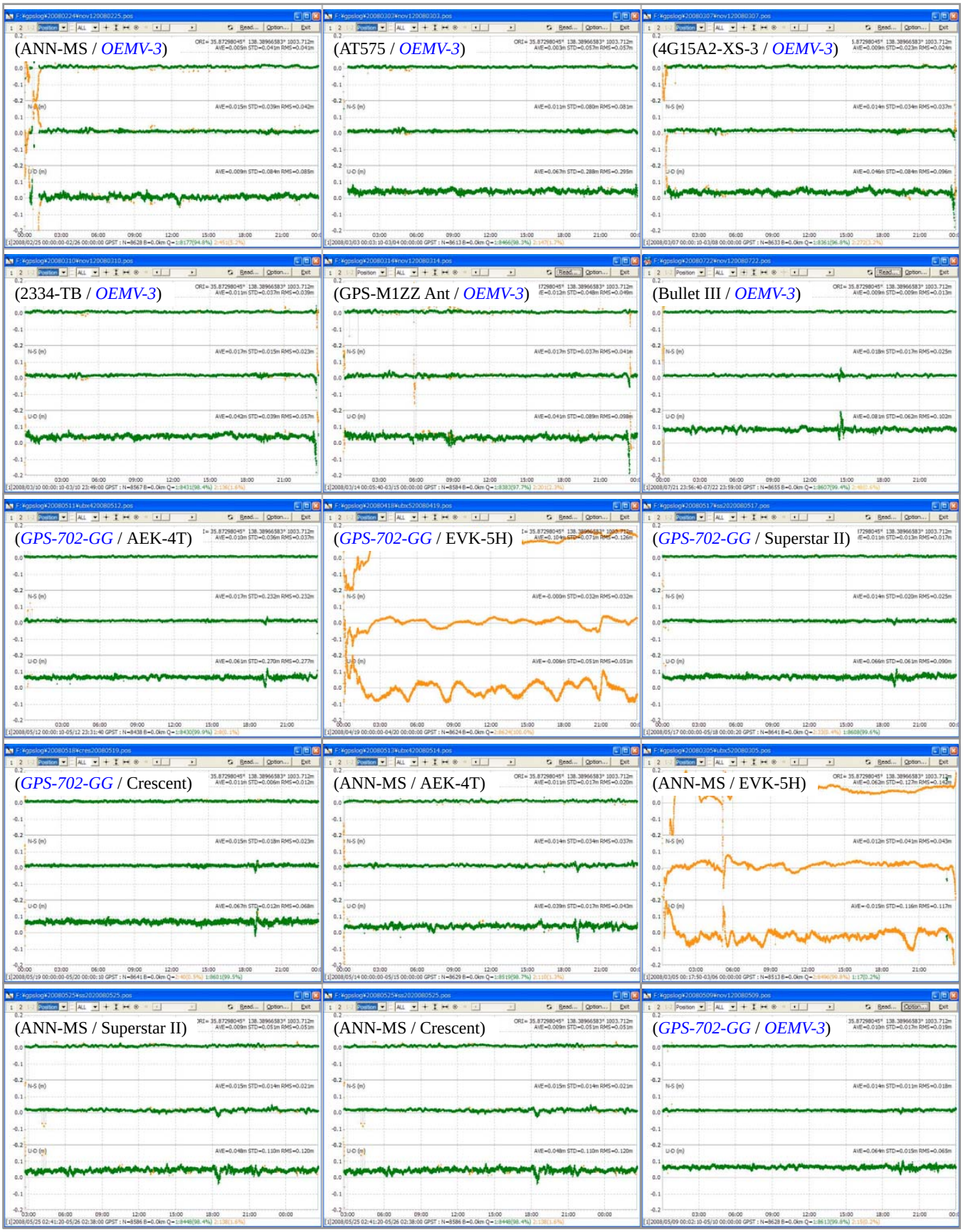

Figure 7. Time series of RTK-GPS positioning errors (antenna / receiver, *italic*: geodetic-grade) (x-axis: time in the range of 0 - 24 hr, y-axes: east/north/up errors in the range of -0.2 to 0.2 m, green: fixed solutions, orange: float solutions)

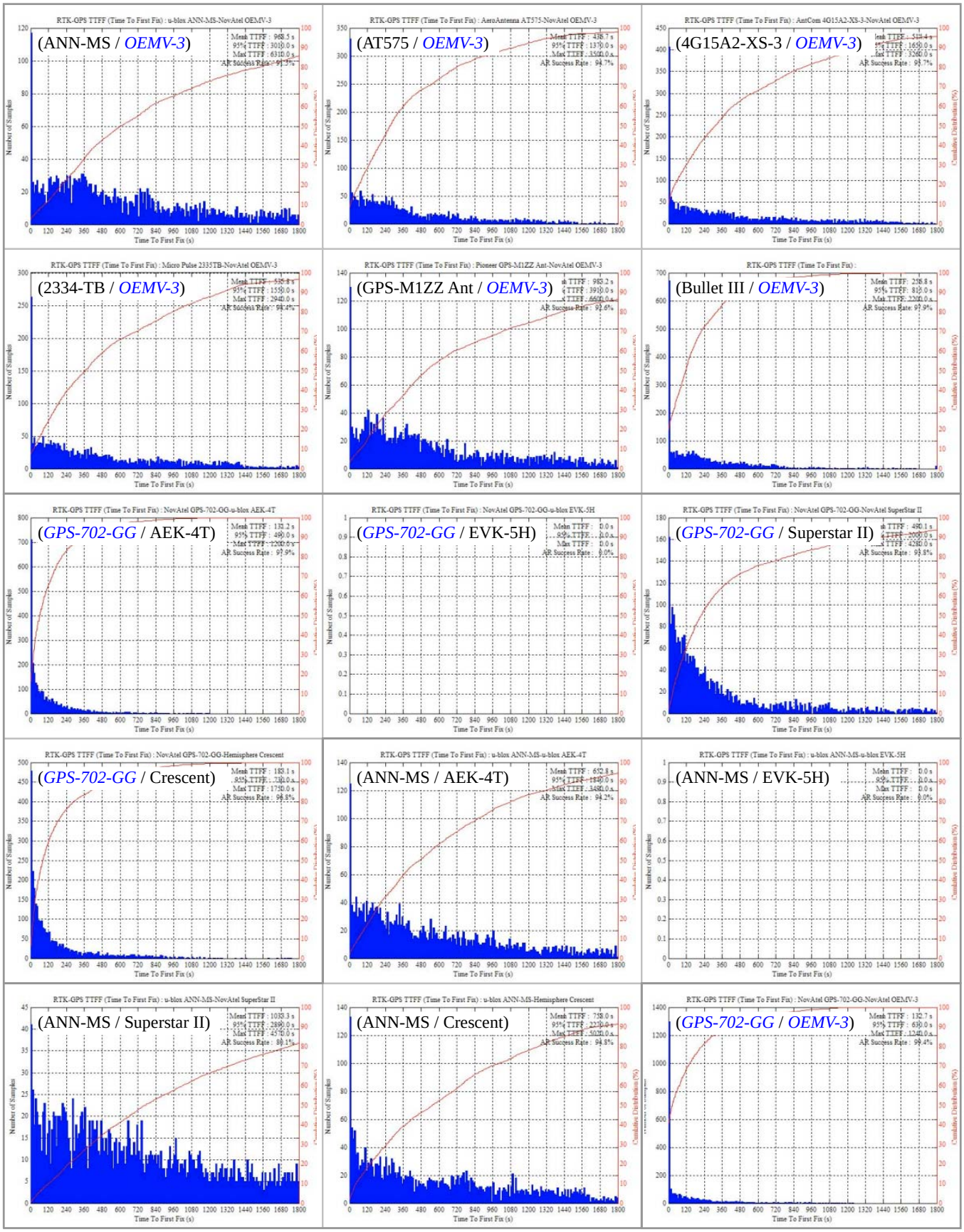

Figure 8. TTFF with ambiguity resolution of RTK-GPS (antenna / receiver, *italic* : geodetic-grade) (x-axis: time in the range of 0 - 1800 s, blue bar: number of samples, red line: cumulative distribution in the range of 0 - 100 %)